Innov Biosyst Bioeng, 2021, vol. 5, no. 2, 85–96
doi: 10.20535/ibb.2021.5.2.230487
UDC 519.2:519.8

Original article

VISIBLE AND REAL SIZES OF NEW COVID-19 PANDEMIC WAVES IN UKRAINE

I. Nesteruk*

[1]Institute of Hydromechanics, National Academy of Sciences of Ukraine, Kyiv, Ukraine
[2]Igor Sikorsky Kyiv Polytechnic Institute, Kyiv, Ukraine

*Corresponding author: inesteruk@yahoo.com

Received 8 April 2021; Accepted 29 April 2021

Background. To simulate the COVID-19 pandemic dynamics, various data sets and different mathematical models can be used. In particular, previous simulations for Ukraine were based on smoothing of the dependence of the number of cases on time, classical and the generalized SIR (susceptible-infected-removed) models. Different simulation and comparison methods were based on official accumulated number of laboratory confirmed cases and the data reported by Johns Hopkins University. Since both datasets are incomplete (a very large percentage of infected persons are asymptomatic), the accuracy of calculations and predictions is limited. In this paper we will try to assess the degree of data incompleteness and correct the relevant forecasts.
Objective. We aimed to estimate the real sizes of two new epidemic waves in Ukraine and compare them with visible dynamics based on the official number of laboratory confirmed cases. We also aimed to estimate the epidemic durations and final numbers of cases.
Methods. In this study we use the generalized SIR model for the epidemic dynamics and its known exact solution. The known statistical approach is adopted in order to identify both the degree of data incompleteness and parameters of SIR model.
Results. We have improved the method of estimating the unknown parameters of the generalized SIR model and calculated the optimal values of the parameters. In particular, the visibility coefficients and the optimal values of the model parameters were estimated for two pandemic waves in Ukraine occurred in December 2020–March 2021. The real number of cases and the real number of patients spreading the infection versus time were calculated. Predictions of the real final sizes and durations of the pandemic in Ukraine are presented. If current trends continue, the end of the pandemic should be expected no earlier than in August 2022.
Conclusions. New method of the unknown parameters identification for the generalized SIR model was proposed, which allows estimating the coefficients of data incompleteness as well. Its application for two pandemic waves in Ukraine has demonstrated that the real number of COVID-19 cases is approximately four times higher than those shown in official statistics. Probably, this situation is typical for other countries. The reassessments of the COVID-19 pandemic dynamics in other countries and clarification of world forecasts are necessary.
Keywords: COVID-19 pandemic; epidemic dynamics in Ukraine; mathematical modeling of infection diseases; SIR model; parameter identification; statistical methods.

Introduction

The studies of the COVID-19 pandemic dynamics are complicated by incomplete information about the number of patients (e.g., reported by WHO [1]), a very large percentage of whom are asymptomatic. In the early stages of the pandemic, there was also a lack of tests and knowledge about the specifics of the infection spread. Because of this, there are more and more evidences of COVID-19 patient appearances before the first officially-confirmed cases [2–6]. These hidden periods of the epidemics in different countries and regions were estimated in [7, 8] with use of the classical SIR model [9–11] and the statistics-based method of the parameter identification developed in [12, 13]. In particular, first COVID-19 cases probably have appeared already in August 2019 [7, 8].

For Ukraine, different simulation and comparison methods were based on official accumulated number of laboratory confirmed cases [14, 15] (these figures coincided with the official WHO data sets [1], but WHO stopped to provide the daily information in August 2020) and the data reported by Johns Hopkins University (JHU) [16]. In particular simple comparisons of epidemic outbreaks in Ukraine neighboring countries can be found in [17]. The classical SIR model was used in [7, 8, 18]. The weakening of quarantine restrictions, changes in the social behavior and the coronavirus activity caused changes in the epidemic dynamics and corresponding parameters of models.

To detect and simulate these new epidemic waves, a simple method of numerical differentiations of the smoothed number of cases and generalized SIR model were proposed and used in [8]. In particular, nine epidemic waves in Ukraine were calculated [8, 19]. Since the Ukrainian national statistics does not look complete (see, e.g., the results of total staff testing in two schools and two children gardens in the Ukrainian city of Chelnytskii, [20]), there is a need to assess the extent of this incompleteness and determine the true sizes of the COVID-19 epidemic in Ukraine, which became the subject of this article.

Data

We will use the data set regarding the accumulated numbers of confirmed COVID-19 cases in Ukraine from national sources [14, 15]. The corresponding numbers V_j and moments of time t_j (measured in days) are shown in Table 1. It must be noted that this table does not show all the COVID-19 cases occurred in Ukraine. Many infected persons are not identified, since they have no symptoms. For example, employees of two kindergartens and two schools in the Ukrainian city of Chmelnytskii were tested for antibodies to COVID-19 [20]. In total 292 people work in the surveyed institutions. Some of the staff had already fallen ill with COVID-19 or were hospitalized. Therefore, they were tested and registered accordingly. In the remaining tested 241 educators, antibodies were detected in 148. Therefore, the number of identified patients (51) in these randomly selected institutions was 3.9 times less than the actual number (51 + 148) of COVID-19 cases.

Many people know that they are ill, since they have similar symptoms as other members of families, but avoid making tests. Unfortunately, one laboratory confirmed case can correspond to

Table 1: Cumulative numbers of laboratory confirmed Covid-19 cases in Ukraine *Vj* according to the national statistics [14, 15]

Day (t_j)	Number of cases (V_j)			
	December 2020	January 2021	February 2021	March 2021
1	758264	1069517	1223879	1357470
2	772760	1074093	1227164	1364705
3	787891	1078251	1232246	1374762
4	801716	1083585	1237169	1384917
5	813306	1090496	1241479	1394061
6	821947	1099493	1244849	1401228
7	832758	1105169	1246990	1406800
8	845343	1110015	1249646	1410061
9	858714	1115026	1253055	1416438
10	872228	1119314	1258094	1425522
11	885039	1124430	1262867	1438468
12	894215	1130839	1268049	1451744
13	900666	1138764	1271143	1460756
14	909082	1146963	1273475	1467548
15	919704	1154692	1276618	1477190
16	931751	1160682	1280904	1489023
17	944381	1163716	1287141	1504076
18	956123	1167655	1293672	1519926
19	964448	1172038	1299967	1535218
20	970993	1177621	1304456	1546363
21	979506	1182969	1307662	1554256
22	989642	1187897	1311844	1565732
23	1001132	1191812	1317694	1579906
24	1012167	1194328	1325841	1596575
25	1019876	1197107	1333844	1614707
26	1025989	1200883	1342016	1632131
27	1030374	1206412	1347849	1644063
28	1037362	1211593	1352134	1652409
29	1045348	1216278	–	1662942
30	1055047	1219455	–	1674168
31	1064479	1221485	–	1691737

several other cases which are not confirmed and displayed in the official statistics. The number of cases in Ukraine reported by COVID-19 Data Repository by the Center for Systems Science and Engineering (CSSE) at Johns Hopkins University (JHU) [16] is 2-3% higher than the Ukrainian national statistics [14, 15] yields (see [19]). Nevertheless, the special simulations will demonstrate a significant incompleteness of both data sets.

Generalized SIR model

The classical SIR model for an infectious disease [9–11] was generalized in [21] to simulate different epidemic waves. We suppose that the SIR model parameters are constant for every epidemic wave, i.e. for the time periods:

$$t_i^* \le t \le t_{i+1}^*, \; i = 1, 2, 3, \ldots$$

Than for every wave we can use the equations, similar to [9–11]:

$$\frac{dS}{dt} = -\alpha_i SI, \tag{1}$$

$$\frac{dI}{dt} = \alpha_i SI - \rho_i I, \tag{2}$$

$$\frac{dR}{dt} = \rho_i I. \tag{3}$$

Here S is the number of susceptible persons (who are sensitive to the pathogen and **not protected**); I is the number of infected persons (who are sick and **spread the infection**); and R is the number of removed persons (who **no longer spread the infection**; this number is the sum of isolated, recovered, dead, and infected people who left the region). It should be noted that the same person can re-enter group S, having been during the previous waves in group R. This happens in the case of re-infection, which is typical of the COVID-19 pandemic.

Parameters α_i and ρ_i are supposed to be constant for every epidemic wave. Values α_i show how quick the susceptible persons become infected (see (1)). These parameters accumulate many characteristics. First they shows how strong (virulent) is the pathogen and what is the way of its spreading. Parameters α_i accumulate also the frequency of contacts and the way of contacting. In order to decrease the values of α_i, we have to minimize the number of our contacts and change our contacting habits. For example, we have to avoid the public places and use masks there, minimize or cancel traveling. We have to change our contact habits: to avoid handshakes and kisses. First, all these simple things are very useful to protect yourself. In addition, if most people follow these recommendations, we have chance to diminish the values of parameters α_i and reduce the negative effects of the pandemic. According to (3) the values ρ_i show the patient removal rates. Then, the inverse values $1/\rho_i$ are the estimations for time of spreading infection τ_i during i-th epidemic wave. So, we are interested in increasing the values of parameters ρ_i and decreasing $1/\rho_i$. People and public authorities should work on this and organize immediate isolation of suspicious cases.

Since the derivative $d(S+I+R)/dt$ is equal to zero (it follows from summarizing Eqs. (1)–(3)), the sum

$$N_i = S + I + R \tag{4}$$

must be constant for every wave. Many articles and books state that the sum $S+I+R$ is equal to the volume of population N_{pop}. Eq. (4) demonstrates once again that this statement is incorrect, since this sum can be different for different epidemic waves in the same population. Some relationships between N_{pop} and N_1 were discussed in [22] for the fist COVID-19 pandemic waves in different countries and regions.

To determine the initial conditions for the set of equations (1)–(3), let us suppose that at the beginning of every epidemic wave t_i^*:

$$I(t_i^*) = I_i, \; R(t_i^*) = R_i, \; S(t_i^*) = N_i - I_i - R_i. \tag{5}$$

In [21] the set of differential equations (1)–(3) was solved by introducing the function

$$V(t) = I(t) + R(t), \tag{6}$$

corresponding to the number of victims or the cumulative confirmed number of cases. For many epidemics (including the COVID-19 pandemic) we cannot observe dependencies $S(t), I(t)$ and $R(t)$. But observations of the accumulated number of cases V_j corresponding to the moments of time t_j provide information for direct assessments of the dependence $V(t)$. The corresponding analytical formulas for this exact solution (taking into account initial conditions (5)) can be written as follows [21]:

$$F_i^*(V, N_i, I_i, R_i, \nu_i) = \alpha_i(t - t_i^*), \quad (7)$$

$$F_i^* = \int_{R_i+I_i}^{V} \frac{dU}{(N_i - U)W_i(U)}, \quad (8)$$

$$W_i(U) = \nu_i \ln(N_i - U) + U - R_i - \nu_i \ln(N_i - R_i - I_i)$$

$$S = N_i - V, R = V - I. \quad (9)$$

Thus, for every set of parameters N_i, I_i, R_i, ν_i and a fixed value of V, integral (8) can be calculated and the corresponding moment of time can be determined from (7). Then functions $I(t)$ and $R(t)$ can be easily calculated with the use of formulas (9). The saturation levels $S_{i\infty}$; $V_{i\infty} = N_i - S_{i\infty}$ (corresponding to the infinite time moment) and the final day of the i-th epidemic wave (corresponding to the moment of time when the number of persons spreading the infection will be less then 1) can be calculated with the use of equations available in [21].

Parameter identification procedure

In the case of a new epidemic, the values of its parameters are unknown and must be identified with the use of limited data sets. For the second and next epidemic waves ($i > 1$), the moments of time t_i^* corresponding to their beginning are known. Therefore the exact solution (7)–(9) depend only on five parameters – $N_i, I_i, R_i, \nu_i, \alpha_i$, when the registered number of victims V_j is a random realization of its theoretical dependence (6). If we assume, that data set V_j is incomplete and there is a constant coefficient $\beta_i \geq 1$, relating the registered and real number of cases during the i-th epidemic wave:

$$V(t_j) \cong \beta_i V_j, \quad (10)$$

the number of unknown parameters increases by one.

Then the values V_j, corresponding to the moments of time t_j, and relationship (10) can be used in eq. (8) in order to calculate $F_{i,j} = F_i^*(V_j, N_i, \nu_i, I_i, R_i, \beta_i)$ for every fixed values of $\beta_i, N_i, \nu_i, I_i, R_i$ and then to check how the registered points fit the linear dependence (7) which can be rewritten as follows:

$$y \equiv F_i^*(V, N_i, I_i, R_i, \nu_i, \beta_i) = \gamma t + \theta, \quad \gamma = \alpha_i, \ \theta = -\alpha_i t_i^*. \quad (11)$$

We can calculate the parameters γ and θ, by treating the values $y_j \equiv F_i^*(V_i, N_i, I_i, R_i, \nu_i, \beta_i)$ and corresponding time moments t_j as random variables. Then we can use the observations of the accumulated number of cases and the linear regression in order to calculate the coefficients $\hat{\gamma}$ and $\hat{\theta}$ of the regression line

$$\hat{y} = \hat{\gamma} t + \hat{\theta} \quad (12)$$

using the standard formulas (see, e.g., [23]). Values $\hat{\gamma}$ and $\hat{\theta}$ from eq. (12) can be treated as statistics-based estimations for parameters γ and θ from relationships (11).

The reliability of the method can be checked by calculating the correlation coefficients r_i (see, e.g., [23]) for every epidemic wave and checking how close are their values is to unity. We can use also the F-test [23] for the null hypothesis that says that the proposed linear relationship (11) fits the data set. Similar approach was used in [7, 8, 12, 13, 18, 19, 24, 25]. To calculate the optimal values of parameters $\beta_i, N_i, \nu_i, I_i, R_i$, we have to find the maximum of the correlation coefficient for the linear dependence (11).

The exact solution (7)–(9) allows avoiding numerical solutions of differential equations (1)–(3) and significantly reduces the time spent on calculations. A new algorithm [26] allows estimating the optimal values of SIR parameters for the i-th epidemic wave directly (without simulations of the previous waves). To reduce the number of unknown parameters, we can use the relationship $V_i = I_i + R_i$ which follows from (6) and (10). To estimate the value V_i, we can use the smoothed accumulated number of cases [8]

$$\bar{V}_i = \frac{1}{7} \sum_{j=i-3}^{j=i+3} V_j, \quad (13)$$

and the relationship $V_i \approx \beta_i \bar{V}_i$ following from (10) (i corresponds to the moment of time t_i^*). One more relationship

$$I_i = \frac{1}{\alpha_i (N_i - V_i)} \frac{dV}{dt}\Big|_{t=t_i^*} \quad (14)$$

can be obtained with the use of (4) and formula

$$\frac{dV}{dt} = \alpha_i SI \quad (15)$$

(following from (2) and (3)). To estimate the average number of new cases dV/dt at the moment of time t_i^* in eq. (14), we can use the numerical differentiation of (13):

$$\left.\frac{d\,\bar{V}}{dt}\right|_{t=t_i} \approx \frac{1}{2}(\bar{V}_{i+1} - \bar{V}_{i-1}) \qquad (16)$$

and relationship (10). Thus we have only three independent parameters β_i, N_i and ν_i. To calculate the value of parameter α_i, some iterations can be used (see details in [26]).

Results

First we have used the registered number of cases [14, 15] for SIR simulations of two COVID-19 pandemic waves in Ukraine, i.e. we supposed that $\beta_i = 1$ for $i = 9$ and $i = 10$. For calculations we have used two time periods: T_{c9} – December 11–24, 2020 and T_{c10} – March 7–20, 2021. Corresponding values of V_j and t_j are listed in Table 1, the number of observations $n_i = 14$ in all the cases. The optimal values of parameters and other characteristics of the ninth and tenth COVID-19 pandemic waves are calculated and listed in Table 2. A similar SIR simulation of the 9th epidemic wave in Ukraine has already been reported in [19], but now we have managed to find a new (larger in value) maximum of the correlation coefficient. It can be seen, the optimal values of SIR parameters are very different for two pandemic waves, but the final sizes and the durations are rather close. As of April 6, 2021 the registered number of COVID-19 cases in Ukraine (1,784,579) has already exceeded the saturation level of the tenth epidemic wave $V_{10\infty} = 1{,}783{,}175$ (see last column in Table 2). It means that without strict quarantine and vaccination we can have new epidemic waves and much higher number of cases.

Table 3 illustrates the results of SIR simulations with the non-prescribed values of β_i. The maximum of the correlation coefficients was

Table 2: Visible ninth and tenth COVID-19 pandemic waves in Ukraine. Results of calculations for optimal values of SIR parameters and other characteristics based on the officially registered number of cases only ($\beta_i = 1$)

Characteristics	9th epidemic wave, $i = 9$	10th epidemic wave, $i = 10$
Time period taken for calculations T_{ci}	December 11–24, 2020	March 11–24, 2021
I_i	148,390.742887927	64,355.4797884056
R_i	732,364.542826359	1,374,292.66306874
N_i	2,960,000	1,792,222.22222222
ν_i	2,275,096.81932990	111544.458681424
α_i	3.48830042313868e-08	4.01417611687886e-07
ρ_i	0.0793622119754996	0.0447759102009153
$1/\rho_i$	12.6004552432172	22.3334376791643
r_i	0.998201733486790	0.998330523577409
$S_{i\infty}$	1,530,454	9,047
$V_{i\infty}$	1,429,546	1,783,175
Final day of the epidemic wave	April 17, 2022	March 29, 2022

Table 3: Real characteristics of ninth and tenth COVID-19 pandemic waves in Ukraine. Results of calculations for optimal values of β_i, SIR parameters, and other characteristics

Characteristics	9th epidemic wave, $i = 9$	10th epidemic wave, $i = 10$
Time period taken for calculations T_{ci}	December 11–24, 2020	March 11–24, 2021
β_i	4.1024	3.7
I_i	668,766.512528977	238,115.275217095
R_i	2,944,443.97158531	5,084,882.85335433
N_i	12,307,200	6,631,222.22222222
ν_i	9626720.00517470	412,714.497121260
α_i	7.59399763733452e-09	1.08491246402134e-07
ρ_i	0.0731052889745776	0.0447759102009154
$1/\rho_i$	13.6789008569236	22.3334376791643
r_i	0.998205208046402	0.998330523577460
$S_{i\infty}$	6,372,870	33,474
$V_{i\infty}$	5,934,330	6,597,748
Final day of the epidemic wave	July 24, 2022	August 16, 2022

achieved at $\beta_9 = 4.1024$ and $\beta_{10} = 3.7$ for ninth and tenth epidemic waves, respectively. These results testify that the main part of the epidemic in Ukraine is invisible. The real numbers of COVID-19 cases are probably approximately 4 times higher than registered ones. The real final size of the tenth epidemic wave $V_{10\infty}$ is expected to be around 6.6 million. Unfortunately, we cannot expect for the end of the pandemic before August 2022 (if vaccinations will not change this sad trend).

As in the case of $\beta_i = 1$, the optimal values of SIR model parameters are very different for ninth and tenth epidemic waves. For example, α_9 is more than 10 times smaller than α_{10}. It means that the pathogen transmission rate has increased drastically. Probably new, more virulent strains of coronavirus have begun to spread widely in Ukraine. They could also change the nature of the course of the disease. In particular, Tables 2 and 3 show that for the tenth wave, the estimate of the average duration of the infection spread $\tau_i = 1/\rho_i$ increased sharply.

Knowing the optimal values of parameters, the corresponding SIR curves can be easily calculated with the use of exact solution (7)–(9) and compared with the pandemic observations before and after corresponding T_{ci}. The results are shown in the Figure by black and blue lines for ninth and tenth waves, respectively. The solid lines show complete accumulated number of cases (visible and invisible); the dashed lines represent the complete number of infected persons multiplied by 5, i.e. $I(t)\times 5$; dotted black lines represent the derivative dV/dt (which is an estimation of the real daily number of new cases) calculated with the use of (15) and multiplied by 100; the black and blue dashed-dotted lines show the dependences $I(t)/\beta_9$ and $I(t)/\beta_{10}$, respectively. "Circles" and "stars" correspond to the accumulated numbers of cases registered during periods of time taken for SIR simulations T_{ci} and beyond these time periods, respectively (taken from Table 1).

Black and blue crosses illustrate the estimations of the real average number of new daily cases for ninth and tenth waves, since the corresponding values were calculated by multiplying the derivative (16) by $100\beta_9$ and $100\beta_{10}$, respectively. Figure shows that stable increase in the daily number of cases occurred after February 12, 2021. This may be due to the abolition of the national lockdown on January 24, 2021, the start of classes in schools and universities, as well as the beginning of the spread of more virulent strains of the coronavirus. The crosses follow very good the theoretical black and blue dotted lines (showing the same derivatives calculated with the use of relationship (15)) for the time periods close to T_{ci}, but deviate significantly during the transition from the ninth to the tenth epidemic wave. These facts indicate the adequacy of the generalized SIR model and method of determining the optimal values of parameters that provide constant values of all coefficients during

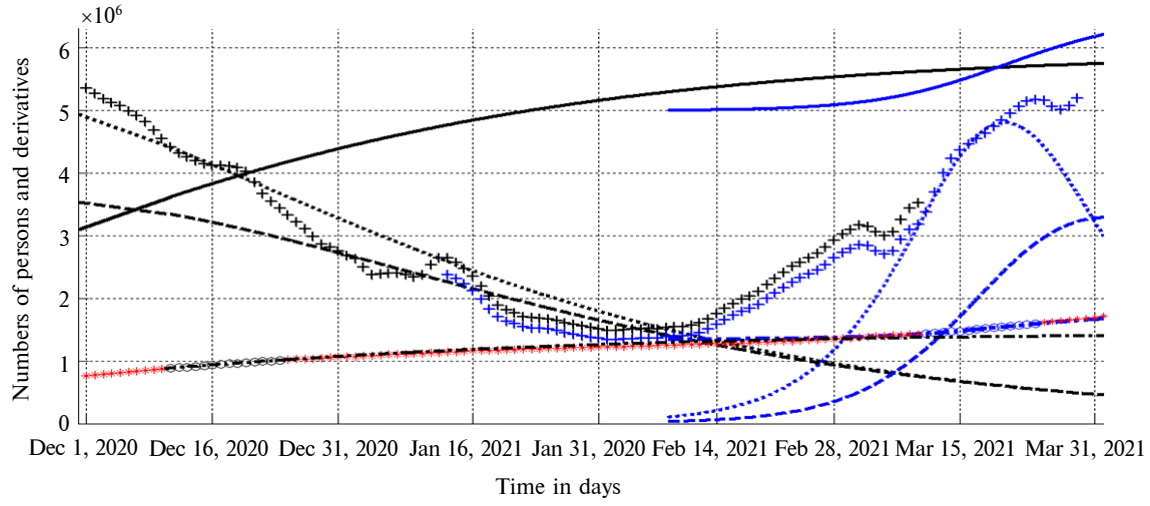

Figure: Real COVID-19 epidemic dynamics in Ukraine. Ninth and tenth waves are shown by black and blue lines, respectively (calculated with the use of the optimal SIR parameters shown in Table 3). Numbers of victims $V(t) = I(t) + R(t)$ – solid lines; numbers of infected and spreading $I(t)$ multiplied by 5 – dashed; derivatives dV/dt (eq. (15)) multiplied by 100 – dotted; dependences $I(t)/\beta_9$ and $I(t)/\beta_{10}$ – black and blue dashed-dotted lines, respectively. "Circles" correspond to the accumulated numbers of cases taken for calculations (during periods of time T_{ci}); "stars" – number of cases beyond T_{ci} (all values from Table1). The black and blue "crosses" show derivative (16) multiplied by $100\beta_9$ and $100\ \beta_{10}$, respectively

the period of time used to calculate them. It should be noted that our attempts to determine the optimal values of the model parameters using data in the transition period (February 12–25, 2021) were unsuccessful (failed to find the maximum correlation coefficient).

In the theoretical estimations for the tenth pandemic wave, the number of persons spreading the infection diminishes drastically in January 2021 (see the dashed blue line in the Figure). In particular, $I = 1$ at the time moment corresponding to January 23, 2021. This fact can be treated as the estimation of beginning of the circulation of a new strain (or strains) of coronavirus, which became dominant in late March 2021. The blue dotted line shows that the real number of new daily cases (estimated with the use of (15)) started to diminish in late March 2021. We don't see this tendency for the registered number of cases (see blue crosses). Probably, the visibility of the epidemic has increased (more real cases started to appear in the official statistics) or there were some changes in the coronavirus activity. Further observations of the pandemic dynamics will show what exactly caused the differences. New calculations using more recent datasets may be required.

Discussion

According to the results of our study, we can only say that in the case of suitability of the generalized SIR model, the values of β_i and other optimal values of its parameters (given in Table 3) are the most reliable (provide the maximum values of the correlation coefficients). Therefore, we used additional methods to verify the calculations and showed some results in Fig. The black and blue dashed-dotted lines represent dependences $I(t)/\beta_i$ which must be close to the registered number of cases (red stars). The coincidence is very good for corresponding epidemic waves.

The calculated coefficients of epidemic visibility $\beta_9 = 4.1024$ and $\beta_{10} = 3.7$ correlate with the results of testing employees of two kindergartens and two schools in the Ukrainian city of Chmelnytskii [20] which revealed the value 3.9. Probably that large discrepancy between registered and actual number of cases occurred not only in Ukraine. For example, total testing in Slovakia (65.5% of population was tested on October 31–November 1, 2020) revealed a number of previously undetected cases, equal to about 1% of the population [27]. On November 7 next 24% of the population was tested and found 0.63% of those infected [28]. According to the WHO report at the end of October, the number of detected cases in Slovakia was also approximately 1% of population [1].

The knowing of real sizes of the COVID-19 pandemic is very important not only from the theoretical point of view. For example, the information about the real dependence $I(t)$ is important to estimate the probability of meeting an infected person with the use of simple formula [29]:

$$p(t) = \frac{I(t)}{N_{\text{pop}}}. \qquad (17)$$

As of March 31, 2021 the theoretical estimations (with the use of parameters presented in the last column of Table 3) yield the value $I = 655380$ (see the blue dashed line in Fig.). Then the probability p can be estimated as 0.015 for Ukraine. If only officially registered cases are taken into account, the corresponding probability will be approximately four times lower. Knowing the real value of probability p is very important for people who are forced to have a lot of contacts, since for M contacts, the probability of meeting at least one infected increases according to the formula [29]:

$$P = 1 - (1 - p)^M \approx pM.$$

Real number of infected people and formula (17) can be useful for deciding which countries' citizens are welcome guests after the resumption of international passenger traffic. If $p_A(t) > p_B(t)$ for countries A and B, citizens of A are not welcome guests in country B at the moment of time t. Many authors are and will be trying to predict the COVID-19 pandemic dynamics in many countries and regions (see, e.g., [2, 4, 6–8, 13, 17–19, 30–93]). The results of this study indicate that reliable estimates of the dynamics require consideration of incomplete data and constant changes of the conditions (quarantine restrictions, social distancing, coronavirus mutations, etc.).

Conclusions

The parameter identification procedure for generalized SIR model was improved in order to estimate the coefficients of data incompleteness. Its application for two pandemic waves in Ukraine has demonstrated that the real number of COVID-19 cases is approximately four times higher than those confirmed by tests and shown in official statistics. Probably, this situation is typical for other countries (with their own values of visibility coefficients). The reassessments of the COVID-19 pandemic dynamics

in other countries and clarification of world forecasts are necessary, since knowing the real sizes of the pandemic is very important to make decisions about quarantine restrictions and vaccination rates.

Acknowledgements

The author is grateful to Oleksii Rodionov for his help in collecting and processing data.

References

[1] Coronavirus Disease (COVID-19) Situation Reports [Internet]. Who.int. 2021 [cited 2021 Apr 6]. Available from: https://www.who.int/emergencies/diseases/novel-coronavirus-2019/situation-reports/

[2] Li Q, Guan X, Wu P, Wang X, Zho L, Tong Y, et al. Early transmission dynamics in Wuhan, China, of novel coronavirus–infected pneumonia. New Engl J Med. 2020;382:1199-207. DOI: 10.1056/NEJMoa2001316

[3] Italian doctors saw 'strange pneumonia' in Lombardy in November [Internet]. South China Morning Post. 2021 [cited 2021 Apr 6]. Available from: https://www.scmp.com/news/china/society/article/3076334/coronavirus-strange-pneumonia-seen-lombardy-november-leading

[4] Lescure F, Bouadma L, Nguyen D, Parisey M, Wicky P, Behillil S, et al. Clinical and virological data of the first cases of COVID-19 in Europe: a case series. Lancet Infect Dis. 2020;20(6):697-706. DOI: 10.1016/S1473-3099(20)30200-0

[5] Militärweltspiele in Wuhan: „Wir sind alle erkrankt" [Internet]. FAZ.NET. 2021 [cited 2021 Apr 6]. Available from: https://m.faz.net/aktuell/sport/mehr-sport/militaerweltspiele-2019-in-wuhan-damals-schon-corona-faelle-16758894.html

[6] Weinberger DM, Cohen T, Crawford FW, Mostashari F, Olson D, Pitzer VE, et al. Estimating the early death toll of COVID-19 in the United States. medRxiv [Preprint] 2020. DOI: 10.1101/2020.04.15.20066431

[7] Nesteruk I. Simulations and predictions of COVID-19 pandemic with the use of SIR model. Innov Biosyst Bioeng. 2020;4(2):110-21. DOI: 10.20535/ibb.2020.4.2.204274

[8] Nesteruk I. COVID-19 pandemic dynamics. Singapore: Springer; 2021. DOI: 10.1007/978-981-33-6416-5

[9] Kermack WO, McKendrick AG. A Contribution to the mathematical theory of epidemics. J Royal Stat Soc Ser A. 1927;115:700-21.

[10] Murray JD. Mathematical biology I/II. New York: Springer; 2002.

[11] Langemann D, Nesteruk I, Prestin J. Comparison of mathematical models for the dynamics of the Chernivtsi children disease. Math Comp Simul. 2016;123:68-79. DOI: 10.1016/j.matcom.2016.01.003

[12] Nesteruk I. Statistics based models for the dynamics of Chernivtsi children disease. Naukovi Visti NTUU KPI. 2017;5:26-34. DOI: 10.20535/1810-0546.2017.5.108577

[13] Nesteruk I. Statistics-based predictions of coronavirus epidemic spreading in mainland China. Innov Biosyst Bioeng. 2020;4(1):13-8. DOI: 10.20535/ibb.2020.4.1.195074

[14] Coronavirus in Ukraine - Statistics [15.03.2021] - Map of infections, graphs [Internet]. Index.minfin.com.ua. 2021 [cited 2021 Apr 6]. Available from: https://index.minfin.com.ua/ua/reference/coronavirus/ukraine/

[15] Cabinet of Ministers of Ukraine – Home [Internet]. Kmu.gov.ua. 2021 [cited 2021 Apr 6]. Available from: https://www.kmu.gov.ua/

[16] COVID-19 Data Repository by the Center for Systems Science and Engineering (CSSE) at Johns Hopkins University [Internet]. GitHub. 2021 [cited 2021 Apr 6]. Available from: https://github.com/owid/covid-19-data/tree/master/public/data

[17] Nesteruk I, Kydybyn I, Demelmair G. Global stabilization trends of COVID-19 pandemic. KPI Sci News. 2020;2:55-62. DOI: 10.20535/kpi-sn.2020.2.205124

[18] Nesteruk I. Dynamics of the coronavirus pandemic in Italy and some global predictions. J Allergy Infect Dis. 2020;1(1):5-8.

[19] Nesteruk I, Benlagha N. Predictions of COVID-19 pandemic dynamics in Ukraine and Qatar based on generalized SIR model. Innov Biosyst Bioeng. 2021;5(1):37-46. DOI: 10.20535/ibb.2021.5.1.228605

[20] An experiment with mass testing for COVID-19 was conducted in Khmelnytsky| Podillya News [Internet]. Podillya News | News of Khmelnytsky region. 2021 [cited 2021 Mar 4]. Available from: https://podillyanews.com/2020/12/17/u-shkolah-hmelnytskogo-provely-eksperyment-z-testuvannyam-na-covid-19

[21] Nesteruk I. General SIR model and its exact solution. In: COVID-19 pandemic dynamics. Singapore: Springer; 2021. DOI: 10.1007/978-981-33-6416-5_9

[22] Nesteruk I. Comparison of the first waves of the COVID-19 pandemic in different countries and regions. In: COVID-19 Pandemic Dynamics. Singapore: Springer; 2021. DOI: 10.1007/978-981-33-6416-5_7

[23] Draper NR, Smith H. Applied regression analysis. 3rd ed. John Wiley; 1998.

[24] Gazzola M, Argentina M, Mahadevan L. Scaling macroscopic aquatic locomotion. Nature Physics. 2014;10:758-61. DOI: 10.1038/nphys3078

[25] Nesteruk I. Maximal speed of underwater locomotion. Innov Biosyst Bioeng. 2019;3(3):152-67. DOI: 10.20535/ibb.2019.3.3.177976

[26] Nesteruk I. Procedures of parameter identification for the waves of epidemics. In: COVID-19 pandemic dynamics. Singapore: Springer; 2021. DOI: 10.1007/978-981-33-6416-5_10

[27] Slovakia tested most of the country in two days. Here's how they did it and what they found [Internet]. CNN. 2021 [cited 2021 Apr 6]. Available from: https://edition.cnn.com/2020/11/02/europe/slovakia-mass-coronavirus-test-intl/index.html

[28] Slovakia's Second Round of Coronavirus Tests Draws Large Crowds [Internet]. Voice of America. 2021 [cited 2021 Apr 6]. Available from: https://www.voanews.com/covid-19-pandemic/slovakias-second-round-coronavirus-tests-draws-large-crowds

[29] Nesteruk I. Classical SIR model and the exact solution of differential equations. In: COVID-19 pandemic dynamics. Singapore: Springer; 2021. DOI: 10.1007/978-981-33-6416-5_4

[30] Wu JT , Leung K_, Leung GM. Nowcasting and forecasting the potential domestic and international spread of the 2019-nCoV outbreak originating in Wuhan, China: A modelling study. Lancet. 2020;395(10225):689-97. DOI: 10.1016/S0140-6736(20)30260-9

[31] Zhao S, Lin Q, Ran J, Musa SS, Yang G, Wang W, et al. Preliminary estimation of the basic reproduction number of novel coronavirus (2019-nCoV) in China, from 2019 to 2020: A data-driven analysis in the early phase of the outbreak. Int J Infect Dis. 2020 Mar;92:214-7. DOI: 10.1016/j.ijid.2020.01.050

[32] Byass P. Eco-epidemiological assessment of the COVID-19 epidemic in China, January–February 2020. Glob Health Action. 2020;13(1):1760490. DOI: 10.1080/16549716.2020.1760490

[33] Tang B, Bragazzi NL, Li Q, Tang S, Xiao Y, Wu J. An updated estimation of the risk of transmission of the novel coronavirus (2019-nCov). Infect Dis Model. 2020;5:248-55. DOI: 10.1016/j.idm.2020.02.001

[34] Ying L, Gayle AA, Wilder-Smith A, Rocklöv J. The reproductive number of COVID-19 is higher compared to SARS coronavirus. J Travel Med. 2020;27(2):taaa021. DOI: https://doi.org/10.1093/jtm/taaa021

[35] Kucharski AJ, Russell TW, Diamond C, Liu Y, Edmunds J, Funk S, et al. Early dynamics of transmission and control of COVID-19: a mathematical modelling study. Lancet Infect Dis. 2020 May;20(5):553-8. DOI: 10.1016/S1473-3099(20)30144-4

[36] Batista M. Estimation of the final size of the COVID-19 epidemic. medRxiv [Preprint] 2020. DOI: 10.1101/2020.02.16.20023606

[37] Dehning J, Zierenberg J, Spitzner FP, Wibral M, Pinheiro Neto J, Wilczek M, et al. Inferring COVID-19 spreading rates and potential change points for case number forecasts. arXiv [Preprint] 2020. arXiv:2004.01105

[38] Chen Y, Cheng J, Jiang Y, Liu K. A time delay dynamical model for outbreak of 2019-nCoV and the parameter identification. arXiv [Preprint] 2020. arXiv:2002.00418

[39] Peng L, Yang W, Zhang D, Zhuge C, Hong L. Epidemic analysis of COVID-19 in China by dynamical modeling. medRxiv [Preprint] 2020. DOI: 10.1101/2020.02.16.20023465

[40] Chang SL, Harding N, Zachreson C, Cliff OM, Prokopenko M. Modelling transmission and control of the COVID-19 pandemic in Australia. Nat Commun. 2020;11:5710. DOI: 10.1038/s41467-020-19393-6

[41] Maier BF, Brockmann D. Effective containment explains sub-exponential growth in confirmed cases of recent COVID-19 out break in mainland China. Science. 2020;368(6492):742-6. DOI: 10.1126/science.abb4557

[42] Wang L, Zhou Y, He J, Zhu B, Wang F, Tang L, et al. An epidemiological forecast model and software assessing interventions on the COVID-19 epidemic in China. Journal of Data Science. 2021;18(13):409-32. DOI: 10.6339/JDS.202007_18(3).0003

[43] Chinazzi M, Davis JT, Ajelli M, Gioannini C, Litvinova M, Merler S, et al. The effect of travel restrictions on the spread of the 2019 novel coronavirus (COVID-19) outbreak. Science. 2020;368(6489):395-400. DOI: 10.1126/science.aba9757

[44] Zhang Y, Jiang B,Yuan J, Tao Y. The impact of social distancing and epicenter lockdown on the COVID-19 epidemic in mainland China: A data-driven SEIQR model study. medRxiv [Preprint] 2020. DOI: 10.1101/2020.03.04.20031187

[45] Ghanam R, Boone EL, Abdel-Salam ASG. SEIRD model for Qatar Covid-19 outbreak: A case study. Lett Biomath. 2021;8(1):19-28.

[46] Udomsamuthirun P, Chanilkul G, Tongkhonburi P, Meesubthong C. The reproductive index from SEIR model of Covid-19 epidemic in Asean. medRxiv [Preprint] 2020. DOI: 10.1101/2020.04.24.20078287

[47] Pereira IG, Guerin JM, Silva Júnior AG, Garcia GS, Piscitelli P, Miani A, et al. Forecasting Covid-19 dynamics in brazil: A data driven approach. Int J Environ Res Public Health. 2020 Jul 15;17(14):5115. DOI: 10.3390/ijerph17145115

[48] Linka K, Peirlinck M, Kuhl E. The reproduction number of COVID-19 and its correlation with public health interventions. Comput Mech. 2020;1-16. DOI: 10.1007/s00466-020-01880-8

[49] Distante C, Gadelha Pereira I, Garcia Goncalves LM, Piscitelli P, Miani A. Forecasting Covid-19 outbreak progression in Italian regions: A model based on neural network training from Chinese data. medRxiv [Preprint] 2020. DOI: 10.1101/2020.04.09.20059055

[50] Hamzah F, Binti A, Lau C, Nazri H, Ligot DV, Lee G, Tan CL. CoronaTracker: Worldwide COVID-19 outbreak data analysis and prediction. Bull World Health Organ. 2020. DOI: 10.2471/BLT.20.255695

[51] Fanelli D, Piazza F. Analysis and forecast of COVID-19 spreading in China, Italy and France. Chaos Solitons Fractals. 2020;134:109761. DOI: 10.1016/j.chaos.2020.109761

[52] Liu Z, Magal P, Seydi O, Webb GF. A model to predict COVID-19 epidemics with applications to South Korea, Italy, and Spain. medRxiv [Preprint] 2020. DOI: 10.1101/2020.04.07.20056945

[53] Bastos SB, Cajueiro DO. Modeling and forecasting the early evolution of the Covid-19 pandemic in Brazil. Sci Rep. 2020;10:19457. DOI: 10.1038/s41598-020-76257-1

[54] Grant A. Dynamics of COVID-19 epidemics: SEIR models underestimate peak infection rates and overestimate epidemic duration. medRxiv [Preprint] 2020. DOI: 10.1101/2020.04.02.20050674

[55] Piccolomiini E L, Zama F. Monitoring Italian COVID-19 spread by an adaptive SEIRD model. medRxiv [Preprint] 2020. DOI: 10.1101/2020.04.03.20049734

[56] Bärwolff G. A Contribution to the mathematical modeling of the Corona/COVID-19 pandemic. medRxiv [Preprint] 2020. DOI: 10.1101/2020.04.01.20050229

[57] Distante C, Piscitelli P, Miani A. Covid-19 Outbreak Progression in Italian Regions: Approaching the peak by the end of March in Northern Italy and first week of April in Southern Italy. Int J Environ Res Public Health. 2020 Apr 27;17(9):3025. DOI: 10.3390/ijerph17093025

[58] te Vrugt M, Bickmann J, Wittkowski R. Effects of social distancing and isolation on epidemic spreading: A dynamical density functional theory model. Nat Commun. 2020;11:5576. DOI: 10.1038/s41467-020-19024-0

[59] Yang Z, Zeng Z, Wang K, Wong SS, Liang W, Zanin M, et al. Modified SEIR and AI prediction of the epidemics trend of COVID-19 in China under public health interventions. J Thorac Dis. 2020 Mar;12(3):165-74. DOI: 10.21037/jtd.2020.02.64

[60] Roda WC, Varughese MB, Han D, Li MY. Why is it difficult to accurately predict the COVID-19 epidemic? Infect Dis Model. 2020;5:271-81. DOI: 10.1016/j.idm.2020.03.001

[61] Otunuga OM, Ogunsolu MO. Qualitative analysis of a stochastic SEITR epidemic model with multiple stages of infection and treatment. Infect Dis Model. 2019 Dec 14;5:61-90. DOI: 10.1016/j.idm.2019.12.003

[62] Chatterjee K, Chatterjee K, Kumar A, Shankard S. Healthcare impact of COVID-19 epidemic in India: A stochastic mathematical model. Med J Armed Forces India. 2020;76(2):147-55. DOI: 10.1016/j.mjafi.2020.03.022

[63] Ciufolini I, Paolozzi A. Mathematical prediction of the time evolution of the COVID-19 pandemic in Italy by a Gauss error function and Monte Carlo simulations. Eur Phys J Plus. 2020;135:355. DOI: 10.1140/epjp/s13360-020-00383-y

[64] Annas S, Isbar Pratama M, Rifandi M, Sanusi W, Side S. Stability analysis and numerical simulation of SEIR model for pandemic COVID-19 spread in Indonesia. Chaos Solitons Fractals. 2020;139:110072. DOI: 10.1016/j.chaos.2020.110072

[65] Yadav RP, Verma R. A numerical simulation of fractional order mathematical modeling of COVID-19 disease in case of Wuhan China. Chaos Solitons Fractals. 2020;140:110124. DOI: 10.1016/j.chaos.2020.110124

[66] Ng KY, Gui MM. COVID-19: Development of a robust mathematical model and simulation package with consideration for ageing population and time delay for control action and resusceptibility. Physica D. 2020 Oct;411:132599. DOI: 10.1016/j.physd.2020.132599

[67] Ivorra B, Ferrández MR, Vela-Pérez M, Ramos AM. Mathematical modeling of the spread of the coronavirus disease 2019 (COVID-19) taking into account the undetected infections. The case of China. Commun Nonlinear Sci Numer Simul. 2020;88:105303. DOI: 10.1016/j.cnsns.2020.105303

[68] Tuan NH, Mohammadi H, Rezapour S. A mathematical model for COVID-19 transmission by using the Caputo fractional derivative. Chaos Solitons Fractals. 2020;140:110107. DOI: 10.1016/j.chaos.2020.110107

[69] Sinkala M, Nkhoma P, Zulu M, Kafita D, Tembo R, Daka V. The COVID-19 pandemic in Africa: Predictions using the SIR model. medRxiv [Preprint] 2020. DOI: 10.1101/2020.06.01.20118893

[70] Agbokou K, Gneyou K, Tcharie K. Investigation on the temporal evolution of the covid'19pandemic: prediction for Togo. Open J Math Sci. 2020;4:273-9. DOI: 10.30538/oms2020.0118

[71] Pintér G, Felde I, Mosavi A, Gloaguen R. COVID-19 Pandemic prediction for Hungary; A hybrid machine learning approach. Mathematics. 2020;8:890. DOI: 10.3390/math8060890

[72] Rossman H, Shilo S, Meir T, Gorfine M, Shalit U, Segal E. Patterns of COVID-19 pandemic dynamics following deployment of a broad national immunization program. medRxiv [Preprint] 2021. DOI: 10.1101/2021.02.08.21251325

[73] Furati KM, Sarumi IO, Khaliq AQM. Memory-dependent model for the dynamics of COVID-19 pandemic. medRxiv [Preprint] 2020. DOI: 10.1101/2020.06.26.20141242

[74] Bosch J, Wilson A, O'Neil K, Zimmerman PA. COVID-19 predict - predicting pandemic trends. medRxiv [Preprint] 2020. DOI: 10.1101/2020.09.09.20191593

[75] Asad A, Srivastava S, Verma MK. Evolution of COVID-19 pandemic in India. Trans Indian Natl Acad Eng. 2020 Sep; 1-8. DOI: 10.1007/s41403-020-00166-y

[76] Aries N, Ounis H. Mathematical modeling of COVID-19 pandemic in the African continent. medRxiv [Preprint] 2020. DOI: 10.1101/2020.10.10.20210427

[77] Günther F, Bender A, Katz K, Kuechenhoff H, Hoehle M. Nowcasting the COVID-19 pandemic in Bavaria. Biom J. 2020 Dec. DOI: 10.1002/bimj.202000112

[78] Yang W, Shaff J, Shaman J. COVID-19 Transmission dynamics and effectiveness of public health interventions in New York City during the 2020 Spring pandemic wave. medRxiv [Preprint] 2020. DOI: 10.1101/2020.09.08.20190710

[79] Dickman R. A SEIR-like model with a time-dependent contagion factor describes the dynamics of the Covid-19 pandemic. medRxiv [Preprint] 2020. DOI: 10.1101/2020.08.06.20169557

[80] Kundu LR, Ferdous MZ, Islam US, Sultana M. Forecasting the spread of COVID-19 pandemic in Bangladesh using ARIMA model. medRxiv [Preprint] 2020. DOI: 10.1101/2020.10.22.20217414

[81] Barbastefano R, Carvalho D, Lippi MC, Pastore D. A novel predictive mathematical model for COVID-19 pandemic with quarantine, contagion dynamics, and environmentally mediated transmission. medRxiv [Preprint] 2020. DOI: 10.1101/2020.07.27.20163063

[82] Biswas MHA, Khatun MS, Paul AK, Khatun MR, Islam MA, Samad SA, et al. Modeling the effective control strategy for transmission dynamics of global pandemic COVID-19. medRxiv [Preprint] 2020. DOI: 10.1101/2020.04.22.20076158

[83] Aviv-Sharon E, Aharoni A. Forecasting COVID-19 pandemic severity in Asia. medRxiv [Preprint] 2020. DOI: 10.1101/2020.05.15.20102640

[84] Bannur N, Maheshwari H, Jain S, Shetty S, Merugu S, Raval A. Adaptive COVID-19 Forecasting via Bayesian Optimization. In: Proceedings of 8th ACM IKDD CODS and 26th COMAD; 2020. DOI: 10.1145/3430984.3431047

[85] Honfo SH, Taboe BH, Kakaï RG. Modeling COVID-19 dynamics in the sixteen West African countries. medRxiv [Preprint] 2020. DOI: 10.1101/2020.09.04.20188532

[86] Chruściel PT, Szybka SJ. Universal properties of the dynamics of the Covid-19 pandemics. medRxiv [Preprint] 2020. DOI: 10.1101/2020.08.24.20181214

[87] Reddy BRM, Singh A, Srivastava P. Covid-19 transmission dynamics in India with extended SEIR model. medRxiv [Preprint] 2020. DOI: 10.1101/2020.08.15.20175703

[88] Huang J, Liu X, Zhang L, Yang K, Chen Y, Huang Z, et al. The amplified second outbreaks of global COVID-19 pandemic. medRxiv [Preprint] 2020. DOI: 10.1101/2020.07.15.20154161

[89] Bhanot G, DeLisi C. Analysis of Covid-19 data for eight European countries and the United Kingdom using a simplified SIR Model. medRxiv [Preprint] 2020. DOI: 10.1101/2020.05.26.20114058

[90] Ibrahim MA, Al-Najafi A. Modeling, control, and prediction of the spread of Covid-19 using compartmental, logistic, and gauss models: A case study in Iraq and Egypt. Processes. 2020;8(11):1400. DOI: 10.3390/pr8111400

[91] Perone G. Comparison of ARIMA, ETS, NNAR and hybrid models to forecast the second wave of COVID-19 hospitalizations in Italy. SSRN [Preprint] 2020. DOI: 10.2139/ssrn.3716343

[92] Bueno AM, Batistela CM, Correa DPF, Piqueira JRC. SIRSi compartmental model for COVID-19 pandemic with immunity loss. Chaos Solitons Fractals. 2021 Jan;142:110388. DOI: 10.1016/j.chaos.2020.110388

[93] Fahmya AE, El-desoukya MM, Mohamed ASA. Epidemic Analysis of COVID-19 in Egypt, Qatar and Saudi Arabia using the generalized SEIR model. medRxiv [Preprint] 2020. DOI: 10.1101/2020.08.19.20178129

І.Г. Нестерук

[1]Інститут гідромеханіки НАНУ, Київ, Україна
[2]КПІ ім. Ігоря Сікорського, Київ, Україна

ВИДИМІ ТА РЕАЛЬНІ МАСШТАБИ НОВИХ ХВИЛЬ ПАНДЕМІЇ COVID-19 В УКРАЇНІ

Проблематика. Для моделювання динаміки пандемії COVID-19 можуть бути використані різні набори даних та різні математичні моделі. Зокрема, попередні моделювання для України базувались на згладжуванні залежності кількості випадків від часу, класичних та узагальнених SIR-моделях (сприйнятливі–інфіковані–видалені). Різні методи моделювання та порівняння базувались на офіційних даних про накопичену кількість лабораторно підтверджених випадків і даних, повідомлених Університетом Джона Хопкінса. Оскільки обидва набори даних є неповними (дуже великий відсоток заражених не мають симптомів), то точність розрахунків і прогнозів є обмеженою. У цій роботі ми спробуємо оцінити ступінь неповноти даних і виправити відповідні прогнози.
Мета. Ми оцінюємо реальні розміри двох нових епідемічних хвиль в Україні та порівнюємо їх із видимою динамікою на основі офіційної кількості лабораторно підтверджених випадків. Також ми оцінюємо тривалість епідемії та остаточну кількість випадків.
Методика реалізації. Використано узагальнену SIR-модель для динаміки епідемії та її відомий точний розв'язок. Відомий статистичний підхід застосовано для того, щоб визначити як ступінь неповноти даних, так і параметри SIR-моделі.
Результати. Удосконалено метод оцінки невідомих параметрів узагальненої SIR-моделі та розраховано оптимальні значення параметрів. Зокрема, коефіцієнти видимості та оптимальні значення параметрів моделі оцінено для двох пандемічних хвиль в Україні, що відбулись у грудні 2020–березні 2021 рр. Розраховано часові залежності для реальної кількості випадків та реальної кількості хворих, що поширюють інфекцію. Представлено прогнози реальних кінцевих розмірів і тривалості пандемії в Україні. Якщо поточні тенденції збережуться, закінчення пандемії слід очікувати не раніше серпня 2022 року.

Висновки. Запропоновано новий метод ідентифікації невідомих параметрів для узагальненої SIR-моделі, який дає змогу також оцінити коефіцієнти неповноти даних. Його застосування для двох пандемічних хвиль в Україні продемонструвало, що реальна кількість випадків захворювання на COVID-19 приблизно в чотири рази перевищує показники офіційної статистики. Можливо, така ситуація характерна і для інших країн. Необхідні переоцінка динаміки пандемії COVID-19 в інших країнах й уточнення світових прогнозів.

Ключові слова: пандемія COVID-19; динаміка епідемії в Україні; математичне моделювання інфекційних захворювань; SIR-модель; ідентифікація параметрів; статистичні методи.

И.Г. Нестерук

[1]Институт гидромеханики НАНУ, Киев, Украина
[2]КПИ им. Игоря Сикорского, Киев, Украина

ВИДИМЫЕ И РЕАЛЬНЫЕ МАСШТАБЫ НОВЫХ ВОЛН ПАНДЕМИИ COVID-19 В УКРАИНЕ

Проблематика. Для моделирования динамики пандемии COVID-19 могут использоваться различные наборы данных и различные математические модели. В частности, предыдущее моделирование для Украины основывалось на сглаживании зависимости количества случаев от времени, классической и обобщенной SIR-моделях (восприимчивые–инфицированные–удаленные). Различные методы моделирования и сравнения были основаны на официальных данных о накопленном количестве лабораторно подтвержденных случаев и данных, представленных Университетом Джона Хопкинса. Поскольку оба набора данных неполны (очень большой процент инфицированных людей не имеют симптомов), то точность расчетов и прогнозов ограничена. В этой статье мы постараемся оценить степень неполноты данных и скорректировать соответствующие прогнозы.
Цель. Мы определяем реальные размеры двух новых эпидемических волн в Украине и сравниваем их с видимой динамикой на основе официального количества лабораторно подтвержденных случаев. Также мы оцениваем продолжительность эпидемии и окончательное количество случаев заболевания.
Методика реализации. Использованы обобщенная SIR-модель для динамики эпидемии и ее известное точное решение. Известный статистический подход использован для определения степени неполноты данных и параметров SIR-модели.
Результаты. Усовершенствована методика оценки неизвестных параметров обобщенной SIR-модели, и рассчитаны оптимальные значения параметров. В частности, оценены коэффициенты видимости и оптимальные значения параметров модели для двух волн пандемии в Украине, произошедших в период с декабря 2020 года по март 2021 года. Рассчитаны реальное количество случаев и реальное количество пациентов, распространяющих инфекцию, в зависимости от времени. Представлены прогнозы реальных окончательных размеров и продолжительности пандемии в Украине. Если текущие тенденции сохранятся, окончания пандемии следует ожидать не ранее августа 2022 года.
Выводы. Предложен новый метод идентификации неизвестных параметров для обобщенной SIR-модели, который позволяет также оценивать коэффициенты неполноты данных. Его использование для двух волн пандемии в Украине показало, что реальное количество случаев COVID-19 примерно в четыре раза выше, чем указано в официальной статистике. Возможно, такая ситуация типична и для других стран. Необходимы переоценка динамики пандемии COVID-19 в других странах и уточнение мировых прогнозов.

Ключевые слова: пандемия COVID-19; динамика эпидемии в Украине; математическое моделирование инфекционных заболеваний; SIR-модель; идентификация параметров; статистические методы.